LETTERS
PUBLISHED ONLINE: 8 FEBRUARY 2009 | DOI: 10.1038/NMAT2379
nature materials

Endohedral fullerenes for organic photovoltaic devices

Russel B. Ross[1], Claudia M. Cardona[2], Dirk M. Guldi[3], Shankara Gayathri Sankaranarayanan[3], Matthew O. Reese[4], Nikos Kopidakis[4], Jeff Peet[5], Bright Walker[6], Guillermo C. Bazan[5], Edward Van Keuren[1], Brian C. Holloway[2] and Martin Drees[2]*

So far, one of the fundamental limitations of organic photovoltaic (OPV) device power conversion efficiencies (PCEs) has been the low voltage output caused by a molecular orbital mismatch between the donor polymer and acceptor molecules. Here, we present a means of addressing the low voltage output by introducing novel trimetallic nitride endohedral fullerenes (TNEFs) as acceptor materials for use in photovoltaic devices. TNEFs were discovered in 1999 by Stevenson *et al.*[1]; for the first time derivatives of the TNEF acceptor, $Lu_3N@C_{80}$, are synthesized and integrated into OPV devices. The reduced energy offset of the molecular orbitals of $Lu_3N@C_{80}$ to the donor, poly(3-hexyl)thiophene (P3HT), reduces energy losses in the charge transfer process and increases the open circuit voltage (V_{oc}) to 260 mV above reference devices made with [6,6]-phenyl-C_{61}-butyric methyl ester (C_{60}-PCBM) acceptor. PCEs >4% have been observed using P3HT as the donor material. This work clears a path towards higher PCEs in OPV devices by demonstrating that high-yield charge separation can occur with OPV systems that have a reduced donor/acceptor lowest unoccupied molecular orbital energy offset.

The trimetallic nitride endohedral fullerenes (TNEFs) used in this study are I_h-C_{80} fullerenes incarcerating rare-earth metals bound in a trimetallic nitride cluster. The spherically symmetric C_{80} and trimetallic nitride cluster do not independently exist, but when combined together form a stable molecule. Owing to the large variety of metals that can be used to make the endohedral cluster, these TNEF nanomaterials are multifunctional, and have been sought for their unique properties in applications such as magnetic resonance imaging contrast agents[2] and optoelectronics[3]. Recent theoretical[4] and experimental data[5] suggest that the lowest unoccupied molecular orbital (LUMO) energies for this type of fullerene are much higher than the LUMO energy of empty-cage species with respect to the Fermi level. The higher LUMO provides a path towards higher V_{oc}, and therefore, higher efficiencies in organic photovoltaic (OPV) devices. Here, $Lu_3N@C_{80}$ was chosen because its LUMO energy is closer to the commonly used OPV donor polymer poly(3-hexyl)thiophene's (P3HT) LUMO level than are those of other available fullerenes such as C_{60} (refs 6,7). Photophysics and OPV device measurements demonstrate that the minimum LUMO offset needed for exciton dissociation is satisfied by $Lu_3N@C_{80}$'s LUMO energy[7]. Cyclic voltammetry and Osteryoung square-wave voltammetry (OSWV), shown in Fig. 1 and Table 1, confirm that the reduction potential and therefore the LUMO levels of the $Lu_3N@C_{80}$ and its methano derivatives are 204 and 280 mV, respectively, more negative than that of [6,6]-phenyl-C_{61}-butyric methyl ester (C_{60}-PCBM), the most common fullerene acceptor used in OPV devices so far. The open circuit voltage in OPVs is correlated to the difference between the donor's highest occupied molecular orbital (HOMO) and the acceptor's LUMO (refs 7–10). Therefore, the increase in reduction potential is representative of the expected V_{oc} gain from $Lu_3N@C_{80}$-based OPV devices[9,11].

Similar to empty-cage fullerenes, the solubility of pristine $Lu_3N@C_{80}$ is not high enough for solution processing of OPVs. Thus, an exohedral functionalization of $Lu_3N@C_{80}$ was required to allow its incorporation into solution-processed bulk-heterojunction OPV devices. Here, we report the first methano derivatives of $Lu_3N@C_{80}$ that have been isolated and fully characterized. It is important to emphasize that the chemical reactivity of $Lu_3N@C_{80}$ differs from empty-cage fullerenes. Owing to these differences in reactivity[5,12–14], the standard protocol used for the synthesis of C_{60}-PCBM (ref. 15) had to be significantly modified to obtain the $Lu_3N@C_{80}$-PCBX (X = M, B, H, O) analogues. For example, the reagents had to be increased to 25 times the amounts used for empty-cage fullerenes, the reaction was run at 120 °C instead of 70 °C and the highest yield was obtained after 25 min rather than 22 h, see Fig. 2 and Supplementary Methods. The $Lu_3N@C_{80}$-PCBX family of derivatives—PCBM (methyl), PCBB (butyl), PCBH (hexyl) and PCBO (octyl)—have proven to have thermal stability up to 300 °C in a thermal gravimetric analyser, see Supplementary Fig. S1. The absorption spectra of bare $Lu_3N@C_{80}$ (Fig. 3) resembles closely its PCBX derivatives, which suggests that this class of TNEF derivatives have a fulleroid character[16]. Electrochemical characterization of these $Lu_3N@C_{80}$-PCBX derivatives also showed the kinetically reductive irreversible behaviour of the pristine $Lu_3N@C_{80}$ and they retained the same reduction potential advantage compared to C_{60}-PCBM, but their solubility in organic solvents and miscibility in P3HT varied significantly. The ability to vary the solubility and miscibility by exchanging the X portion of the PCBX functional group on TNEF molecules and not affect the molecular orbitals can serve as a vital tool for designing

[1]Georgetown University, 37th and O st. NW, Washington, District of Columbia 20057, USA, [2]Luna Innovations Incorporated, 521 Bridge Street, Danville, Virginia 24541, USA, [3]Department of Chemistry and Pharmacy & Interdisciplinary Center for Molecular Materials (ICMM), Friedrich-Alexander-Universität Erlangen-Nürnberg, Egerlandstr. 3, 91058 Erlangen, Germany, [4]National Renewable Energy Laboratory, 1617 Cole Blvd, Golden, Colorado 80401, USA, [5]Center for Polymer and Organic Solids, University of California, Santa Barbara, California 93106, USA, [6]Department of Chemistry and Biochemistry (or Center for Polymers and Organic Solids) University of California at Santa Barbara, Santa Barbara, California 93117, USA.
*e-mail: dreesm@lunainnovations.com.

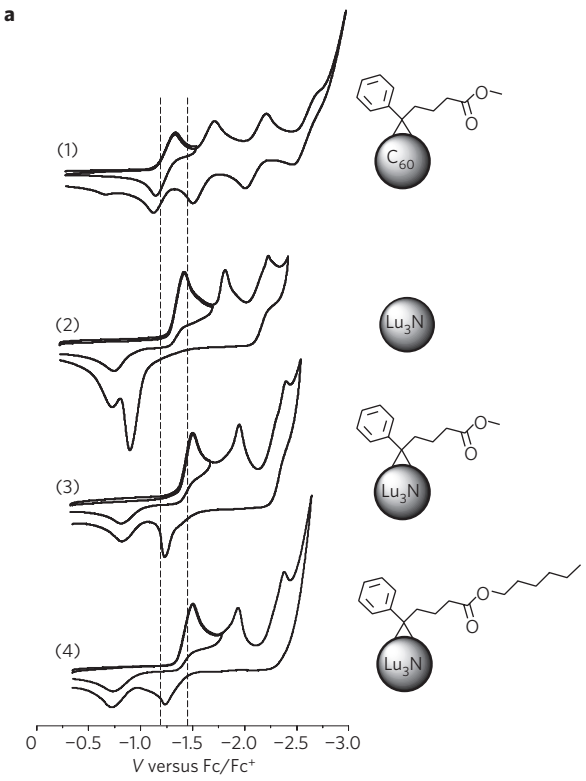

Figure 1 | TNEF electrochemical properties to establish LUMO levels. **a**, Cyclic voltammograms of the reductive behaviour of (1) C_{60}-PCBM, (2) $Lu_3N@C_{80}$, (3) $Lu_3N@C_{80}$-PCBM, (4) $Lu_3N@C_{80}$-PCBH in 0.5 M *n*-Bu_4NPF_6/*o*-DCB (*o*−DCB : 1,2−dichlorobenzene) with ferrocene as the internal standard, 100 mV s^{-1} scan rate. **b**, OSWV measurements of C_{60}-PCBM and $Lu_3N@C_{80}$ in 0.05 M *n*-Bu_4NPF_6/*o*-DCB.

Table 1 | Redox potentials (*V* versus Fc/Fc^+) of the first oxidation and first reduction processes measured by OSWV in 0.05 M *n*-Bu_4NPF_6/*o*-DCB.

	$E_{p,ox(1)}$	$E_{p,red(1)}$
C_{60}-PCBM	+1.132	−1.220
$Lu_3N@C_{80}$	+0.635	−1.424
$Lu_3N@C_{80}$-PCBM	+0.556	−1.510
$Lu_3N@C_{80}$-PCBH	+0.564	−1.500

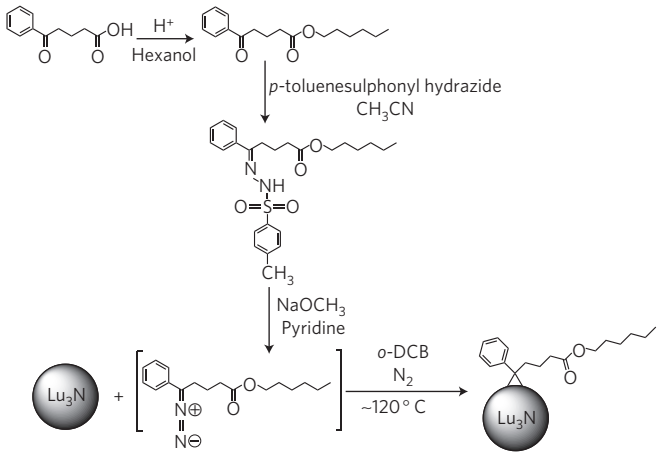

Figure 2 | Synthetic protocol for $Lu_3N@C_{80}$-PCBH.

the optimal composite morphology for high-performance OPV devices. $Lu_3N@C_{80}$-PCBH was chosen among the synthesized $Lu_3N@C_{80}$-PCBX derivatives for this study because of its similarities in solubility and miscibility to C_{60}-PCBM in the processing of P3HT-based OPV devices. Characterization of space-charge-limited devices further confirmed that $Lu_3N@C_{80}$-PCBH possesses similar charge-carrier mobility to C_{60}-PCBM (4.0×10^{-4} for $Lu_3N@C_{80}$-PCBH versus 1.4×10^{-3} $cm^2\,V^{-1}\,s^{-1}$ for C_{60}-PCBM), see Supplementary Fig. S2.

Photophysical studies were carried out to understand the excited-state interaction of the $Lu_3N@C_{80}$ derivatives with the P3HT donor polymer. Charge transfer between photoexcited TNEF and P3HT was confirmed for the first time by means of subnanosecond photolytic experiments. Specifically, we contrasted the photophysical behaviour in spin-coated films with that in solution by exciting either at 387 nm (fullerenes) or at 540 nm (P3HT) and comparing the resulting photospectra with those of the corresponding radical cation and radical anion produced in radiolytic experiments, see Supplementary Fig. S3. Initially the P3HT singlet excited-state features are discernible in photoexcited films of P3HT/$Lu_3N@C_{80}$-PCBH or P3HT/C_{60}-PCBM—see Fig. 4 and Supplementary Fig. S4. However, they are in both cases ultrashort: they decay in less than 550 fs ($>2.0 \times 10^{12}$ M^{-1}) to form a new photoproduct. There is a decisive difference between the photoproducts of the two acceptors: in the near-infrared region, the photoproducts absorb with maxima at 665, 890 and 1,020 nm for P3HT/C_{60}-PCBM and 665, 890 and 1,025 nm for P3HT/$Lu_3N@C_{80}$-PCBH. The first two maxima (665 and 890 nm) are in excellent agreement with those noted for the one-electron oxidized radical cation of P3HT in dichloromethane (600 and 855 nm—Supplementary Fig. S3a); the last ones (1,020 or 1,025 nm) correspond to the one-electron reduced C_{60}-PCBM and $Lu_3N@C_{80}$-PCBH radical anions generated in toluene, acetone and 2-propanol (see Supplementary Fig. S3b). The visible portion of the transient absorption spectra, on the other hand, is in both cases dominated by strong bleaching of the ground state, revealing minima at 500 nm. These fingerprints again corroborate the attributes seen during the P3HT oxidation. In other words, both $Lu_3N@C_{80}$-PCBH and C_{60}-PCBM give rise to the rapid formation of the radical ion pair states, under excitation of either the donor or the acceptor. These radical ion pair states were found to be stable on the timescale of our investigation (up to 3,000 ps). Complementary nanosecond experiments (see Supplementary Fig. S5) confirm the remarkable stability of the radical ion pair states in both films with lifetimes exceeding the experimental time window of our apparatus (1.0 ms). These transient absorption measurements with P3HT/$Lu_3N@C_{80}$-PCBH

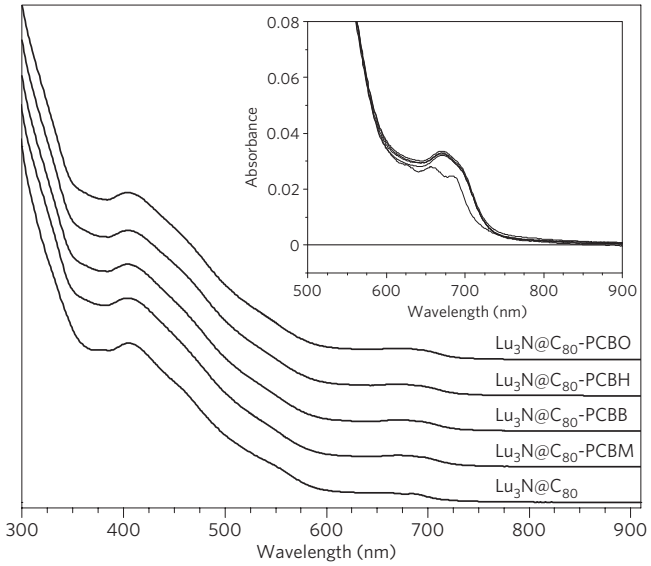

Figure 3 | Absorption spectra of $Lu_3N@C_{80}$ and its methano derivatives. Inset: Spectra for all four methano derivatives with their parent molecule $Lu_3N@C_{80}$ overlaid and magnified in the absorption onset region.

and P3HT/C_{60}-PCBM films on quartz, photoexciting P3HT at 540 nm, revealed the same amplitudes for the P3HT radical cation absorptions at 855 nm, which indicates that the charge transfer process for the $Lu_3N@C_{80}$-PCBH-based film is as efficient as that seen for C_{60}-PCBM. The presented efficiency and stability of the charge-separated states of P3HT/$Lu_3N@C_{80}$-PCBH should yield photocurrent densities in OPV devices that are equal to or greater than the P3HT/C_{60}-PCBM reference system.

OPV devices using a P3HT/$Lu_3N@C_{80}$-PCBH active layer show a significant increase in open circuit voltage compared with P3HT/C_{60}-PCBM reference devices. Figure 5a illustrates the illuminated and dark current density (J) versus voltage (V) curves for an optimized P3HT/$Lu_3N@C_{80}$-PCBH device with a PCE of 4.2%. The measured P3HT/$Lu_3N@C_{80}$-PCBH device has a similar photocurrent and fill factor (FF) to the P3HT/C_{60}-PCBM reference device, thereby demonstrating that the higher V_{oc} of the TNEF-based OPV device leads to a higher PCE. The short-circuit current densities (J_{sc}) of both devices were cross-referenced with an integration of the external quantum efficiency (EQE) measurements. Both of the devices' EQE spectra shown in Fig. 5b integrated within 2% of the measured J_{sc} under solar simulation tests. It is important to note here that there were differences in the fabrication conditions to achieve optimum performance for each of the two devices shown in Fig. 5. The P3HT/C_{60}-PCBM reference film was annealed in an inert atmosphere for 10 min at 150 °C after deposition of a lithium fluoride/aluminium top electrode. The optimal processing for the P3HT/$Lu_3N@C_{80}$-PCBH film was achieved by annealing the film at 110 °C for 10 min before the LiF/Al top electrode was deposited with an extra 30 s anneal at 140 °C after production. The optimal processing of these two devices differs slightly; however, the absorption spectra and grazing incident X-ray diffraction data shown in Fig. 5c,d demonstrate that the blend films are similar in overall absorption and polymer order[17–20]. A 12% lower crystallinity of the P3HT phase has been interpreted from the grazing incident X-ray diffraction data, and is one example of how future devices made with P3HT/$Lu_3N@C_{80}$-PCBH active layers may be improved in J_{sc} and FF. The similar absorption of these two films combined with the magnitude of the extracted photocurrent further validates the charge transfer efficiency of the P3HT/$Lu_3N@C_{80}$-PCBH system measured during photolytic experimentation.

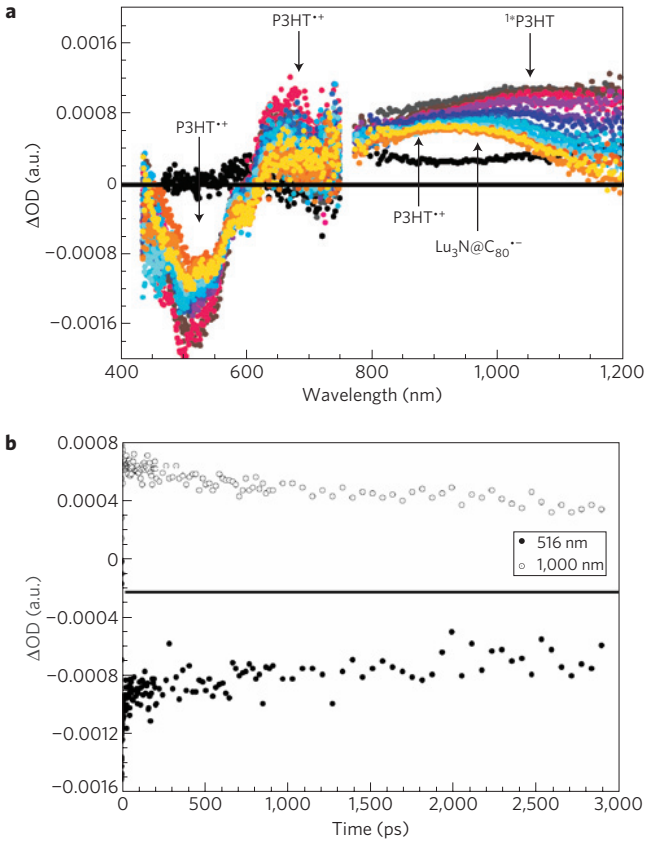

Figure 4 | Time-resolved TNEF photophysics. a, Differential absorption spectra (visible and near-infrared) obtained on femtosecond flash photolysis (387 nm) of a P3HT/$Lu_3N@C_{80}$-PCBH film in air with several time delays between 0 and 50 ps at room temperature—arrows indicate the main characteristics of the P3HT singlet excited state (asterisk) and the radical ion pair state (dot). **b**, Time-absorption profiles of the spectra shown in **a** at 516 nm (filled circles) and 1,000 nm (open circles), monitoring the radical ion pair state.

Open circuit voltages as high as 890 mV ($J_{sc} = 5.4$ mA cm^{-2} and FF = 0.52) have been observed for P3HT/$Lu_3N@C_{80}$-PCBH devices, which is to our knowledge, the highest V_{oc} in P3HT/fullerene OPV devices reported so far. This observed 260 mV V_{oc} enhancement over the P3HT/C_{60}-PCBM reference device is close to the 280 mV increase predicted by electrochemistry. Fluctuations in the P3HT/$Lu_3N@C_{80}$-PCBH devices' V_{oc} from 890 to 810 mV have been attributed to processing-induced surface states at the active layer/cathode interface. Evidence of this surface-state interaction is witnessed in $Lu_3N@C_{80}$-PCBH-based films with variations in film dry times and choice of cathode materials. Films dried in less than two minutes and capped with a LiF/Al cathode exhibit V_{oc} values that approach the maximum predicted V_{oc}, as is demonstrated by the 890 mV device. In contrast, films prepared under similar conditions with a 20 nm calcium/80 nm Al cathode exhibit this increase in V_{oc} with longer dry times (data not shown). In an effort to optimize our PCE and to uncover all of the variables involved in achieving the paramount bulk heterojunction with $Lu_3N@C_{80}$-PCBH, we are further investigating these fluctuations in the P3HT/$Lu_3N@C_{80}$-PCBH device performance that are encountered under different processing techniques. Our results of this work will be addressed in a future publication.

In summary, here we report the first synthesis of $Lu_3N@C_{80}$ methano derivatives and their use as novel acceptor materials in state-of-the-art OPV devices that have an 890 mV open circuit voltage, the highest reported open circuit voltage for a P3HT/fullerene

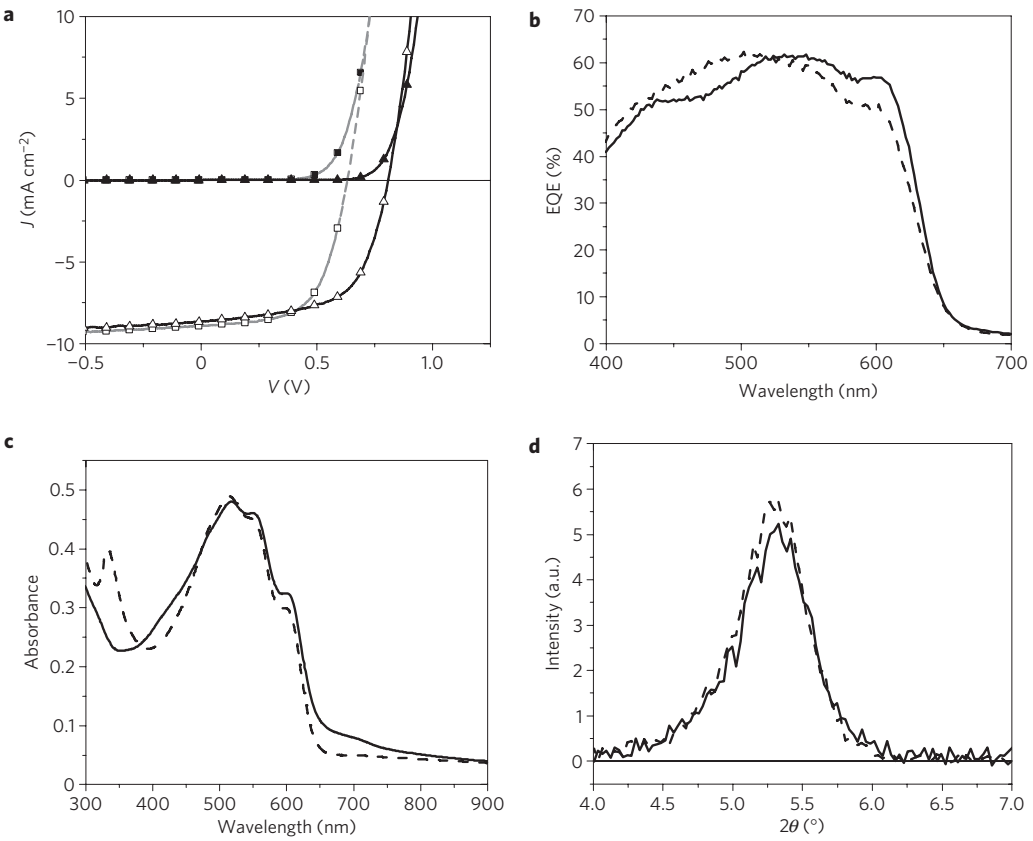

Figure 5 | Blend-film electronic and optical properties. a, *J*–*V* curves of P3HT/$Lu_3N@C_{80}$-PCBH (triangles) PCE = 4.2%, V_{oc} = 810 mV, J_{sc} = 8.64 mA cm^{-2} and FF = 0.61 and P3HT/C_{60}-PCBM (squares and dashed lines) PCE = 3.4%, V_{oc} = 630 mV, J_{sc} = 8.9 mA cm^{-2} and FF = 0.61 blend devices. Filled symbols show the dark curves and open symbols show devices under simulated Air Mass 1.5 (100 mW cm^{-2}). **b**, EQE P3HT/$Lu_3N@C_{80}$-PCBH (dashed) and P3HT/C_{60}-PCBM (solid) blend devices. **c**, Absorption of P3HT/$Lu_3N@C_{80}$-PCBH (solid) and P3HT/C_{60}-PCBM (dashed) blend films. **d**, X-ray diffraction of the P3HT (100) peak normalized to thickness for a 1:1 blend film of P3HT/$Lu_3N@C_{80}$-PCBH (solid) and a 1:0.8 reference film of P3HT/C_{60}-PCBM (dashed) blend.

device. Photophysical experiments confirm the efficient charge transfer between P3HT and the $Lu_3N@C_{80}$-PCBH. Optimization of the P3HT/$Lu_3N@C_{80}$-PCBH active-layer morphology has resulted in OPV devices with higher V_{oc} values and a similar photocurrent and fill factor compared to P3HT/C_{60}-PCBM reference devices. The higher overall PCE of the P3HT/$Lu_3N@C_{80}$-PCBH devices is attributed to a better positioned LUMO level that captures more of the energy associated with each absorbed photon. This work demonstrates that reducing the donor/acceptor LUMO offset by using TNEF acceptor materials can lead to enhanced OPV performance through the V_{oc}. Using the improved LUMO level offset of our $Lu_3N@C_{80}$-PCBH acceptor materials and combining it with previously reported low-bandgap donor polymers[21,22], OPV efficiencies greater than 10% may now be feasible[6,7]. With this we have introduced an entirely new class of acceptor materials for organic solar cells that show a straightforward path towards commercially viable devices.

Received 11 July 2008; accepted 6 January 2009; published online 8 February 2009

References

1. Stevenson, S. *et al.* Small-bandgap endohedral metallofullerenes in high yield and purity. *Nature* **401**, 55–57 (1999).
2. MacFarland, D. K. *et al.* Hydrochalarones: A novel endohedral metallofullerene platform for enhancing magnetic resonance imaging contrast. *J. Med. Chem.* **51**, 3681–3863 (2008).
3. Jones, M. A. G., Taylor, R. A., Ardavan, A., Porfyrakis, K. & Briggs, G. A. D. Direct optical excitation of a fullerene-incarcerated metal ion. *Chem. Phys. Lett.* **428**, 303–306 (2006).
4. Campanera, J. M., Bo, C., Olmstead, M. M., Balch, A. L. & Poblet, J. M. Bonding within the endohedral fullerenes $Sc_3N@C_{78}$ and $Sc_3N@C_{80}$ as determined by density functional calculations and reexamination of the crystal structure of $\{Sc_3N@C_{78}\}\cdot Co(OEP)\cdot 1.5(C_6H_6)\cdot 0.3(CHCl_3)$. *J. Phys. Chem. A* **106**, 12356–12364 (2002).
5. Cardona, C. M., Elliott, B. & Echegoyen, L. Unexpected chemical and electrochemical properties of $M_3N@C_{80}$ (M = Sc, Y, Er). *J. Am. Chem. Soc.* **128**, 6480–6485 (2006).
6. Koster, L. J. A., Mihailetchi, V. D. & Blom, P. W. M. Ultimate efficiency of polymer/fullerene bulk heterojunction solar cells. *Appl. Phys. Lett.* **88**, 0935111 (2006).
7. Scharber, M. C. *et al.* Design rules for donors in bulk-heterojunction solar cells—Towards 10% energy-conversion efficiency. *Adv. Mater.* **18**, 789–794 (2006).
8. Brabec, C. J. *et al.* Origin of the open circuit voltage of plastic solar cells. *Adv. Funct. Mater.* **11**, 374–380 (2001).
9. Kooistra, F. B. *et al.* Increasing the open circuit voltage of bulk-heterojunction solar cells by raising the LUMO level of the acceptor. *Org. Lett.* **9**, 551–554 (2007).
10. Brabec, C. J. *et al.* The influence of materials work function on the open circuit voltage of plastic solar cells. *Thin Solid Films* **403/404**, 368–372 (2002).
11. Lenes, M. *et al.* Fullerene bisadducts for enhanced open-circuit voltages and efficiencies in polymer solar cells. *Adv. Mater.* **20**, 2116–2119 (2008).
12. Campanera, J. M., Bo, C. & Poblet, J. M. Exohedral reactivity of trimetallic nitride template (TNT) endohedral metallofullerenes. *J. Org. Chem.* **71**, 46–54 (2006).
13. Cardona, C. M., Kitaygorodskiy, A. & Echegoyen, L. Trimetallic nitride endohedral metallofullerenes: Reactivity dictated by the encapsulated metal cluster. *J. Am. Chem. Soc.* **127**, 10448–10453 (2005).
14. Rodriguez-Fortea, A., Campanera, J. M., Cardona, C. M., Echegoyen, L. & Poblet, J. M. Dancing on a fullerene surface: Isomerization of $Y_3N@$(N-ethylpyrrolidino-C_{80}) from the 6,6 to the 5,6 regioisomer. *Angew. Chem. Int. Ed.* **45**, 8176–8180 (2006).

15. Hummelen, J. C. *et al.* Preparation and characterization of fulleroid and methanofullerene derivatives. *J. Org. Chem.* **60**, 532–538 (1995).
16. Lukoyanova, O. *et al.* 'Open rather than closed' malonate methano-fullerene derivatives. The formation of methanofulleroid adducts of $Y_3N@C_{80}$. *J. Am. Chem. Soc.* **129**, 10423–10430 (2007).
17. Li, G. *et al.* 'Solvent annealing' effect in polymer solar cells based on poly(3-hexylthiophene) and methanofullerenes. *Adv. Funct. Mater.* **17**, 1636–1644 (2007).
18. Erb, T. *et al.* Correlation between structural and optical properties of composite polymer/fullerene films for organic solar cells. *Adv. Funct. Mater.* **15**, 1193–1196 (2005).
19. Peet, J. *et al.* Method for increasing the photoconductive response in conjugated polymer/fullerene composites. *Appl. Phys. Lett.* **89**, 252105 (2006).
20. Zhokhavets, U., Erb, T., Gobsch, G., Al-Ibrahim, M. & Ambacher, O. Relation between absorption and crystallinity of poly(3-hexylthiophene)/fullerene films for plastic solar cells. *Chem. Phys. Lett.* **418**, 347–350 (2006).
21. Muhlbacher, D. *et al.* High photovoltaic performance of a low-bandgap polymer. *Adv. Mater.* **18**, 2931–2931 (2006).
22. Peet, J. *et al.* Efficiency enhancement in low-bandgap polymer solar cells by processing with alkane dithiols. *Nature Mater.* **6**, 497–500 (2007).

Acknowledgements

This material is based on work supported by the Air Force Office of Scientific Research under Contract No. FA9550-06-C-0010. Any opinion, findings and conclusions or recommendations expressed in this material are those of the authors and do not necessarily reflect the views of the Air Force Office of Scientific Research. This material is also based on work supported by the National Science Foundation under Grant No. 0348955 and Grant No. IIP-0740454. Additional thanks to The Cluster of Excellence 'Engineering of Advanced Materials' and the Alexander von Humboldt Foundation for generous support (S.G.S.).

Additional information

The authors declare competing financial interests: details accompany the full-text HTML version of the paper at www.nature.com/naturematerials. Supplementary Information accompanies this paper on www.nature.com/naturematerials. Reprints and permissions information is available online at http://npg.nature.com/reprintsandpermissions. Correspondence and requests for materials should be addressed to M.D.